

## Basic Study

**Monochromatic energy computed tomography image for active intestinal hemorrhage: A model investigation**

Wen-Dong Liu, Xing-Wang Wu, Jun-Mei Hu, Bin Wang, Bin Liu

Wen-Dong Liu, Xing-Wang Wu, Jun-Mei Hu, Bin Liu, Department of Radiology, the First Affiliated Hospital of Anhui Medical University, Hefei 230022, Anhui Province, China  
Bin Wang, Department of Epidemiology and Statistics, Anhui Medical University, Hefei 230022, Anhui Province, China  
Author contributions: Liu WD, Wu XW contributed equally to this work; Wu XW designed and performed research; Liu WD wrote the paper and analyzed data; Hu JM analyzed data; Liu B provided technical support and revised this paper; Wang B provided statistical support.

**Open-Access:** This article is an open-access article which was selected by an in-house editor and fully peer-reviewed by external reviewers. It is distributed in accordance with the Creative Commons Attribution Non Commercial (CC BY-NC 4.0) license, which permits others to distribute, remix, adapt, build upon this work non-commercially, and license their derivative works on different terms, provided the original work is properly cited and the use is non-commercial. See: <http://creativecommons.org/licenses/by-nc/4.0/>

Correspondence to: Bin Liu, MD, Department of Radiology, the First Affiliated Hospital of Anhui Medical University, Jixi Road, Hefei 230022, Anhui Province, China. [liubin1305@126.com](mailto:liubin1305@126.com)

Telephone: +86-551-62922396

Fax: +86-551-62922396

Received: May 20, 2014

Peer-review started: May 22, 2014

First decision: July 21, 2014

Revised: July 31, 2014

Accepted: September 12, 2014

Article in press: September 16, 2014

Published online: January 7, 2015

**Abstract**

**AIM:** To investigate the value of computed tomography (CT) spectral imaging in the evaluation of intestinal hemorrhage.

**METHODS:** Seven blood flow rates were simulated *in vitro*. Energy spectral CT and mixed-energy CT scans

were performed for each rate (0.5, 0.4, 0.3, 0.2, 0.1, 0.05 and 0.025 mL/min). The detection rates and the contrast-to-noise ratios (CNRs) of the contrast agent extravasation regions were compared between the two scanning methods in the arterial phase (AP) and the portal venous phase (PVP). Comparisons of the CNR values between the PVP and the AP were made for each energy level and carried out using a completely random *t* test. A  $\chi^2$  test was used to compare the detection rates obtained from the two scanning methods.

**RESULTS:** The total detection rates for energy spectral CT and mixed-energy CT in the AP were 88.57% (31/35) and 65.71% (23/35), respectively, and the difference was significant ( $\chi^2 = 5.185$ ,  $P = 0.023$ ); the total detection rates in the PVP were 100.00% (35/35) and 91.4% (32/35), respectively, and the difference was not significant ( $\chi^2 = 1.393$ ,  $P = 0.238$ ). In the AP, the CNR of the contrast agent extravasation regions was  $3.58 \pm 2.09$  on the mixed-energy CT images, but the CNRs were  $8.78 \pm 7.21$  and  $8.83 \pm 6.75$  at 50 and 60 keV, respectively, on the single-energy CT images, which were significantly different ( $3.58 \pm 2.09$  vs  $8.78 \pm 7.21$ ,  $P = 0.031$ ;  $3.58 \pm 2.09$  vs  $8.83 \pm 6.75$ ,  $P = 0.029$ ). In the PVP, the differences between the CNRs at 40, 50 and 60 keV different monochromatic energy levels and the polychromatic energy images were significant ( $19.35 \pm 10.89$  vs  $11.68 \pm 6.38$ ,  $P = 0.010$ ;  $20.82 \pm 11.26$  vs  $11.68 \pm 6.38$ ,  $P = 0.001$ ;  $20.63 \pm 10.07$  vs  $11.68 \pm 6.38$ ,  $P = 0.001$ ). The CNRs at the different energy levels in the AP and the PVP were significantly different ( $t = -2.415$ ,  $-2.380$ ,  $-2.575$ ,  $-2.762$ ,  $-2.945$ ,  $-3.157$ ,  $-3.996$  and  $-3.189$ ).

**CONCLUSION:** Monochromatic energy imaging spectral CT is superior to polychromatic energy images for the detection of intestinal hemorrhage, and the detection was easier in the PVP compared with the AP.

**Key words:** Spectral imaging; Computed tomography; Monochromatic energy imaging; Small bowel bleeding

© The Author(s) 2015. Published by Baishideng Publishing Group Inc. All rights reserved.

**Core tip:** Recent technical advances, including monochromatic energy image spectral computed tomography (CT) with its accurate material-decomposition images and monochromatic spectral images at energy levels, are only rarely included in intestinal hemorrhage studies. This paper aimed to verify the diagnostic value of spectral CT in small bowel bleeding.

Liu WD, Wu XW, Hu JM, Wang B, Liu B. Monochromatic energy computed tomography image for active intestinal hemorrhage: A model investigation. *World J Gastroenterol* 2015; 21(1): 214-220 Available from: URL: <http://www.wjg-net.com/1007-9327/full/v21/i1/214.htm> DOI: <http://dx.doi.org/10.3748/wjg.v21.i1.214>

## INTRODUCTION

Gastrointestinal (GI) bleeding, especially lower GI bleeding, is a critical and sometimes life-threatening condition. Rapid and accurate localization of the bleeding sites and early etiological determination are the focus of clinical investigations, but these factors also represent major clinical challenges. Endoscopy enables the accurate localization and diagnosis in most cases of upper GI bleeding but not in lower GI bleeding<sup>[1]</sup>. Digital subtraction angiography (DSA) has been shown to be effective in the clinical diagnosis of GI bleeding. However, detection and diagnosis often fail in cases of bleeding rates below 0.5 mL/min<sup>[2,3]</sup>. Radioisotope scanning can detect a rate below 0.1 mL/min, but accurate localization is difficult<sup>[4]</sup>. Multidetector row computed tomography (MDCT) technology has recently shown increasingly prominent advantages in the diagnosis of small bowel bleeding<sup>[5]</sup>. Recent technical advances include energy spectral CT with its advantages of enabling monochromatic energy imaging, reduced tissue attenuation, high resolution, and the detection of small changes in tissue density<sup>[6,7]</sup>. Compared with conventional MDCT, energy spectral CT is particularly sensitive regarding the detection of active bleeding in the GI tract. However, the diagnostic value of energy spectral CT in small bowel bleeding has not been previously established. Therefore, this paper aimed to verify the diagnostic value of spectral CT in small bowel bleeding.

## MATERIALS AND METHODS

### Bleeding model

**Microsyringe:** A WZ-50C6 microsyringe produced by Zhejiang University Medical Instrument Co., Ltd. (Hefei Province, China) was used, and the amount injected and the injection rates were calibrated on a regular basis. A 2.5% solution of mannitol (CT value 30-40 HU) was injected into the small bowels of pigs *in vitro*, and the

tissues were immersed in a container of plant oil (30 cm × 15 cm × 10 cm X-ray permeable plastic container). The contrast agent was loaded into the microsyringe (in a proportion of 300 mgI/mL Omnipaque to physiological saline at 1:45, CT value 280-300 HU). Seven bleeding rates were simulated: 0.5, 0.4, 0.3, 0.2, 0.1, 0.05 and 0.025 mL/min.

A 24G indwelling needle connected to one end of the microsyringe was used to penetrate the intestinal wall, and the needle was fixed in place. The contrast agent was injected at the seven rates mentioned above.

### CT scanning

Single-energy spectral CT (GE Discovery HD750 CT scanner) and poly-chromatic energy CT (GE Light Speed 64 VCT) were employed. For each bleeding rate, the scans were repeated five times. Following each scan, the liquid in the intestinal canal was replaced. The gemstone spectral imaging (GSI) platform was used for image reconstruction in the standard reconstruction mode. The CT images obtained using the seven monochromatic energy images (40-100 keV with a 10 keV interval) and the polychromatic energy images (120 kVp) were analyzed. The delays used were 15 and 40 s.

The following scanning parameters in the conventional mode (polychromatic energy CT) were used: 120 kV, 300 mA, pitch 0.984, collimation 40 mm, gantry rotation time 0.8 s, slice thickness 5 mm, and eight slices scanned. The following scanning parameters in the GSI mode (helical 0.5 s, 40 mm) were used: 80/140 kV, 0.5 ms instant switching, pitch 0.984, gantry rotation time 0.8 s, slice thickness 5 mm, and eight slices scanned.

### Data acquisition

The contrast-to-noise ratios (CNRs) were determined (*i.e.*, the CNRs of the iodine-containing region and the surrounding water-containing region in the intestinal canal). The layers that exhibited clear extravasation of the contrast agent were selected on the polychromatic energy images and the seven monochromatic energy images. Regions of interest with identical size and morphology were selected. According to the equation,  $CNR = (|CT1 - 2|)/SD$ ; thus, the CNRs for the extravasation regions under the different bleeding rates were calculated. CT1 is the CT value of the region of contrast agent extravasation, CT2 is the CT value of the liquid in the intestinal canal of the same layer, and SD is the standard deviation of the CT attenuation value of the water environment in the intestinal canal of the same layer.

**Image quality scoring:** Based on the length of the contrast agent column and the CT value, the image quality was classified into five levels: 5 points, clearly displayed contrast agent column (length ≥ 2 cm or CT value ≥ 150 HU); 4 points, visible contrast agent column (length 1-2 cm or CT value 100-150 HU); 3 points, obscure contrast agent column (length ≤ 1 cm or CT value ≤ 100 HU); 2 points, no visible contrast agent column; and 1 point, no contrast agent imaging. Two radiologists

**Table 1** Comparison of detection rates for the region of contrast agent exudation between spectral computed tomography and multidetector row computed tomography in different phases

Grouping	Detection result		Total	Detection rate	$\chi^2$	P value
	Detected	Not detected				
64-slice CT in the AP	23	12	35	65.71%	5.185	0.023
spectral CT in the AP	31	4	35	88.57%		
64-layer CT in the PVP	32	3	35	91.43%	1.393 <sup>1</sup>	0.238
spectral CT in PVP	35	0	35	100.00%		

<sup>1</sup>Represent  $\chi^2$  correction. 64-layer computed tomography (CT) in arterial phase (AP) and portal venous phase (PVP),  $\chi^2 = 6.873$ ,  $P = 0.009$ ; spectral CT in AP and PVP,  $\chi^2$  corrected = 2.386,  $P = 0.122$ .

who were blinded to the experimental parameters independently evaluated the image quality. A discussion was required to reach a consensus when their opinions were inconsistent.

### Statistical analysis

SPSS 17.0 (SPSS, Inc., Chicago, United States) was used. The quantitative data are expressed as the mean  $\pm$  SD. A randomized block analysis of the variance was performed on the CNRs of the images obtained under the seven energy levels and their quality scores. Each pair of energy levels was compared using the Bonferroni method. The CNRs and the image quality scores between the portal venous phase (PVP) and the arterial phase (AP) were compared for each energy level using a completely random *t* test. The detection rates for the energy spectral CT and the 64-slice CT were compared using the  $\chi^2$  test, and  $P < 0.05$  indicated significance.

## RESULTS

There were differences in the detection rates for the regions of contrast agent extravasation using the two scanning methods in different phases.

### AP

Of the 35 spectral CT scans, the extravasation region was detected in 31 scans. Using 64-slice CT scanning, the extravasation region was detected in 23 scans. The detection rates of the spectral and 64-slice CT scanning were 88.57% (31/35) and 65.71% (23/35), respectively, and the difference was significant ( $\chi^2 = 5.185$ ,  $P = 0.023$ ).

### PVP

The detection rates of the spectral and 64-slice CT scanning were 100.00% (35/35) and 91.43% (32/35), respectively, and the difference was not significant ( $\chi^2 = 1.393$ ,  $P = 0.238$ ). The detection rates in the PVP and AP were significantly different when 64-slice CT scanning was used ( $\chi^2 = 6.873$ ,  $P = 0.009$ ), whereas the difference was not significant when spectral CT scanning was used ( $\chi^2$  corrected = 2.386,  $P = 0.122$ ) (Table 1). When the bleeding rate decreased to 0.025 mL/min, the detection rate in the AP with 64-slice CT scanning was zero, and it was 60% (3/5) in the PVP; the detection rate with spectral CT scanning was 60% (3/5) in the AP and 100% (5/5) in the

PVP. When the bleeding rate was high, both 64-slice and spectral CT scanning facilitated the easy detection of the regions of extravasation. The optimal monochromatic energy images obtained using spectral CT scanning exhibited clearer extravasation regions. When the bleeding rate was 0.5 mL/min, the 60 keV images were superior compared with the 100 keV images and the polychromatic energy images (Figure 1). When the bleeding rate decreased to 0.05 and 0.025 mL/min, 64-slice CT scanning did not facilitate the detection of the extravasation region in the AP. However, the extravasation region was clearly visualized in the PVP. When spectral CT scanning at 50 keV was used, the extravasation region was clearly visualized in both the PVP and the AP (Figure 1E).

There were differences in the CNRs for the two scanning methods at each energy level in the PVP and the AP.

The CNRs of the extravasation region obtained with spectral CT scanning at 50 and 60 keV in the AP were  $8.78 \pm 7.21$  and  $8.83 \pm 6.75$ , respectively; compared with the CNRs obtained with polychromatic energy CT scanning ( $3.58 \pm 2.09$ ), the difference was significant ( $P < 0.05$ ). In the PVP, the CNRs for monochromatic energy images at 40, 50 and 60 keV were  $19.35 \pm 10.89$ ,  $20.82 \pm 11.26$  and  $20.63 \pm 10.07$ , respectively. These values were significantly different compared with polychromatic energy CT scanning ( $11.68 \pm 6.38$ ,  $P < 0.05$ ). The CNRs for a given energy level in the AP and PVP were significantly different ( $t = -2.415, -2.380, -2.575, -2.762, -2.945, -3.157, -3.996$  and  $-3.189$ ) ( $P < 0.05$ ) (Table 2).

There were differences in the image quality score at each energy level in the PVP and the AP using the two scanning methods.

The differences in the PVP between 40, 50 and 60 keV were not significant. However, the image quality at each of these three energy levels was significantly different compared with the polychromatic energy images ( $P < 0.05$ ). The differences in the AP between 40, 50 and 60 keV were not significant, but the differences among the other energy levels were all significant ( $P < 0.05$ ). The quality scores of the monochromatic energy images at 40, 50 and 60 keV were slightly higher compared with the polychromatic energy images in both phases (Table 3).

## DISCUSSION

MDCT has been shown to be effective for the visualiza-

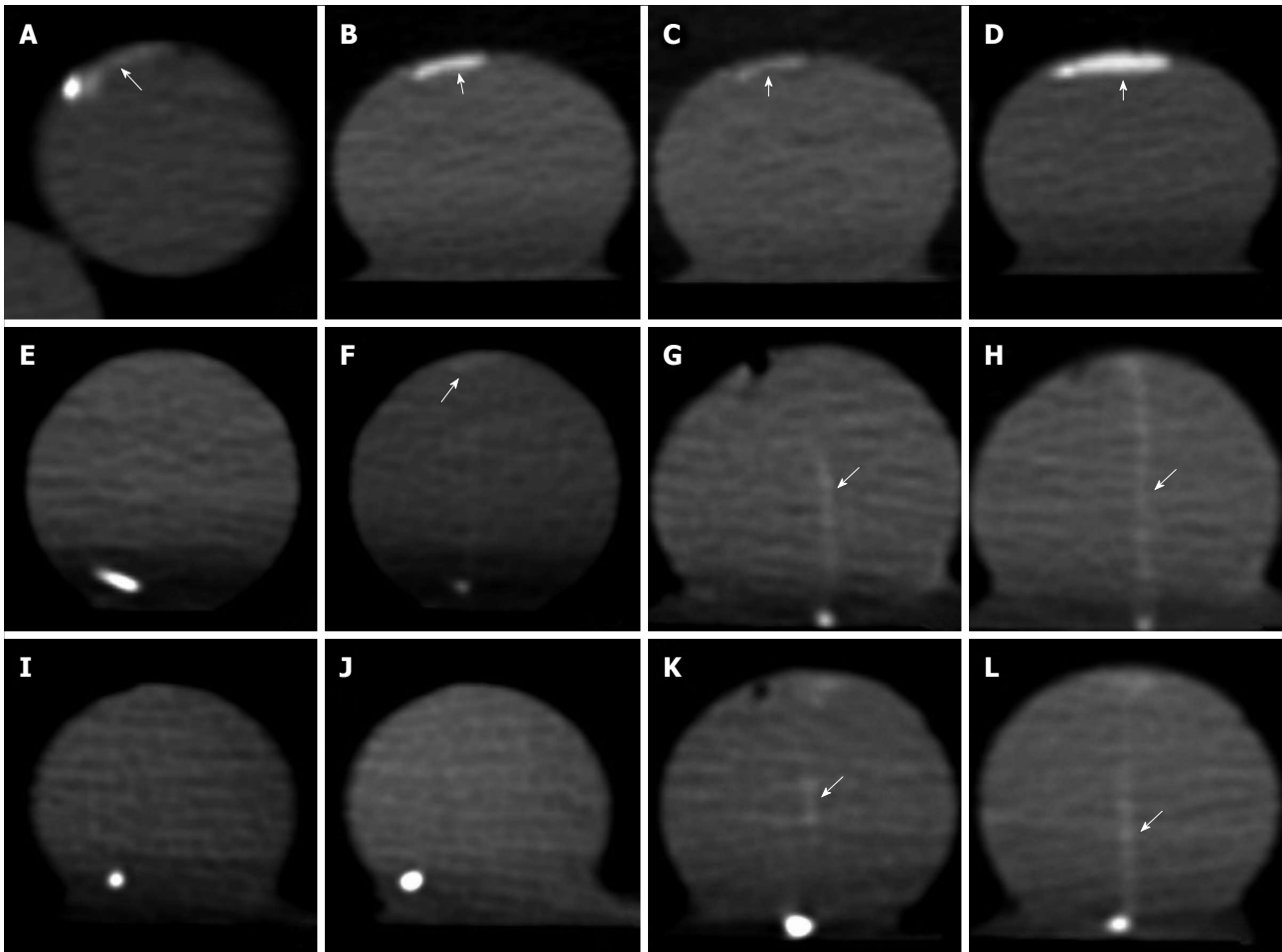


**Figure 1** Computed tomography scan. A: Image of 64-slice computed tomography (CT) scan at 0.5 mL/min in the arterial phase (arrow) (AP); B, C: Monochromatic energy images at 60 and 100 keV in the AP at 0.5 mL/min, which are clearer than the polychromatic energy images (arrow) (A); D: Monochromatic energy image at 60 keV in the portal venous phase (arrow) (PVP) at 0.5 mL/min, which is more clear than that in the AP (B); E, F: Images at 64-slice CT scan in the AP and (arrow) PVP at 0.05 mL/min. No region of exudation could be observed in the AP, but it was observed vaguely in the PVP; G, H: Images at 50 keV monoenergetic energy in the AP and PVP (arrow) at 0.05 mL/min, which are much clearer than those obtained by 64-slice CT scan (E, F); I, J: Images at 64-slice CT scan in the AP and PVP at 0.025 mL/min, on which no exudation region could be detected; K, L: Monochromatic energy images at 50 keV in the AP and PVP (arrow) at 0.025 mL/min, on which the exudation regions can be clearly seen.

**Table 2** Comparison of contrast to noise ratios values of the exudation regions at each energy level and blood flow rate between portal venous phase and arterial phase

	PVP	AP	<i>t</i>	<i>P</i> value
40 keV	19.35 ± 10.89	7.69 ± 6.68	-2.415 <sup>1</sup>	0.036
50 keV	20.82 ± 11.26	8.78 ± 7.21	-2.380	0.035
60 keV	20.63 ± 10.07	8.83 ± 6.75	-2.575	0.024
70 keV	15.65 ± 8.17	5.93 ± 4.46	-2.762	0.017
80 keV	10.46 ± 5.83	3.44 ± 2.41	-2.945	0.012
90 keV	7.33 ± 3.92	2.31 ± 1.52	-3.157	0.008
100 keV	5.83 ± 2.70	1.49 ± 1.01	-3.996	0.004
Mixed-energy image	11.68 ± 6.38	3.58 ± 2.09	-3.189	0.015
<i>F</i>	18.298	7.823		
<i>P</i> value	0.000	0.000		

<sup>1</sup>Using Satterthwaite's approximate *t* test. No significant difference between 40, 50, 60 and 70 keV in the portal venous phase (PVP), but the difference was significant when compared with the polychromatic energy imaging (*P* < 0.05). No significant difference between 40, 50 and 60 keV in the arterial phase (AP), but the difference was significant when compared with the polychromatic energy imaging (*P* < 0.05).

tion of small hemorrhages in the GI tract because of the sub-millimeter scanning ability and the powerful image post-processing<sup>[8-11]</sup>. When the bleeding rate is greater than 0.5 mL/min, the detection rate using MDCT can reach 93%<sup>[12]</sup>. Monochromatic energy imaging combined with the use of iodine-based contrast materials leads to an increased ability of single-energy spectral CT to detect small hemorrhages in the GI tract compared with conventional MDCT<sup>[13,14]</sup>. In this study, a GE HD750 CT scanner was used for gemstone spectral imaging to confirm its diagnostic value in cases of active bleeding in the GI tract. The results provide the basis for the clinical selection of a more simple and effective tool for the localization of small intestine bleeding sites.

The comparison of the monochromatic and polychromatic energy images demonstrated that when the bleeding rate was high, both spectral CT and MDCT scanning facilitates the easy detection of the regions of contrast agent extravasation. However, when the bleeding

**Table 3** Comparison of image quality scores at each energy level and blood flow rate between portal venous phase and arterial phase

	PVP	AP	<i>t</i>	<i>P</i> value
40 keV	4.63 ± 0.58	3.46 ± 1.43	1.999 <sup>1</sup>	0.081
50 keV	4.46 ± 0.65	3.06 ± 1.20	2.724	0.018
60 keV	4.20 ± 0.77	2.97 ± 1.26	2.195	0.049
70 keV	3.54 ± 0.91	2.23 ± 0.92	2.692	0.020
80 keV	3.00 ± 0.83	1.97 ± 0.87	2.263	0.043
90 keV	2.46 ± 0.55	1.49 ± 0.49	3.494	0.004
100 keV	2.26 ± 0.54	1.09 ± 0.11	5.650 <sup>1</sup>	0.001
Mixed-energy imaging	3.60 ± 1.13	2.46 ± 1.06	1.953	0.074
<i>F</i>	52.549	19.875		
<i>P</i> value	0.000	0.000		

<sup>1</sup>Using Satterthwaite's approximate *t* test. There was no significant difference between 40, 50 and 60 keV in the portal venous phase (PVP), but the difference was significant when compared with the polychromatic energy imaging (*P* < 0.05). There was no significant difference between 40, 50 and 60 keV in the arterial phase (AP), but the difference was significant among other energy levels (*P* < 0.05).

rate decreased, the difficulty of detecting the extravasation regions increased accordingly. The use of monochromatic energy imaging facilitated the observation of the regions of contrast agent extravasation, thereby significantly increasing the detection rates. When the bleeding rate decreased below a specific level, the extravasation region may not have been detected in the AP, but it was always successfully detected in the PVP. Dobritz *et al.*<sup>11</sup> also reported that when the bleeding rate was low, the region of extravasation was not detected in some cases in the AP. Because of the increased concentration of the contrast agent in the PVP, the detection rate was substantially higher.

The detection rates in the PVP and the AP using 64-slice CT scanning were significantly different, and the detection rate was higher in the PVP. However, no difference was detected with the use of spectral CT scanning, although this finding might be related to the limited sample size. Yamaguchi *et al.*<sup>15</sup> demonstrated that the detection rate obtained with MDCT during active bleeding of the GI tract could reach 80%, and the sensitivity and specificity of CT angiography were 89% and 85%, respectively<sup>15,16</sup>. The detection rate with DSA averaged 47% (range: 27%-77%), as reported in the literature. The sensitivity, specificity and accuracy of DSA in the detection of small bowel bleeding were 91.7%, 100% and 92%, respectively<sup>17-19</sup>. The detection rates using spectral CT scanning in this study were 88.57% (31/35) and 100% (35/35) in the AP and the PVP, respectively. These values were substantially higher compared with previous reports, which suggest that spectral CT is superior for the detection of active bleeding in the small intestines. It may be employed as the primary choice in clinical practice to produce a higher detection rate.

The optimal monochromatic energy value for the detection of the extravasation region on monochromatic energy images: Compared with the MDCT images, the monochromatic energy images had a higher image qual-

ity and higher signal-to-noise ratios and CNRs. Single-energy spectral CT integrates single-energy imaging and iodine-based material decomposition, which provides a new prospect for the development of CT technology<sup>20-23</sup>. Our experiments indicated that the extravasation regions detected on monochromatic energy images varied with the specific energy level in both the AP and the PVP. The image qualities at 50 and 60 keV were substantially better compared with the polychromatic energy images. The average CNRs at 50 and 60 keV in the PVP were 1.78 and 1.76 times higher compared with the polychromatic energy images and 2.45 and 2.47 times higher compared with the AP, respectively. The extravasation regions were visualized more clearly on the monochromatic energy images at 50 and 60 keV compared with the other energy levels or on the polychromatic energy images. The CNRs in the PVP were generally higher compared with the AP. It is clear that 50-60 keV is the optimal energy level. It was demonstrated experimentally that the monochromatic energy images also had a higher quality score compared with the polychromatic energy images at 40, 50 and 60 keV. The optimal energy level provides an image that achieves a balance between tissue contrast and noise level and enables clear visualization of the lesions. Because MDCT is based on polychromatic energy imaging, the CT value of the material is likely to shift, thereby affecting the image quality<sup>24,25</sup>.

Limitations of the present research: (1) the ideal filled state was simulated in the intestinal canal using the established model. However, under clinical conditions, the intestinal canals of some patients may be empty, which affects the detection of active bleeding. Thus, our experiments tended to overestimate the ability of CT to evaluate active bleeding; and (2) the small sample size also affected the precision of the results. Furthermore, these findings must be confirmed in *in vivo* studies.

Monochromatic energy imaging in spectral CT was superior compared with polychromatic energy imaging for the detection of the region of contrast agent extravasation. The optimal energy level was 50-60 keV. For patients with suspected small bowel bleeding, spectral CT at the recommended energy level of 50-60 keV is the first-line choice for diagnosis.

## COMMENTS

### Background

Rapid and accurate localization of the bleeding sites and early etiological determination are the focus of investigation, but also the major challenges. In comparison with conventional multidetector row computed tomography (MDCT), energy spectral CT is particularly sensitive to detect active bleeding in the gastrointestinal (GI). However, the diagnostic value of energy spectral CT in small bowel bleeding has not been established. Therefore, this paper aimed to verify the diagnostic value of spectral CT in small bowel bleeding.

### Research frontiers

GI bleeding, especially lower GI, is a critical and sometimes life-threatening condition. In the area of detecting hemorrhages in the GI, the hotspot is how to find the bleeding sites rapidly and accurately.

### Innovations and breakthroughs

MDCT has been proved to be effective in visualizing tiny hemorrhages in the

GI, owing to the sub-millimeter scanning ability and the powerful image post-processing. When the bleeding rate is over 0.5 mL/min, the detection rate by MDCT can reach 93%. The mono-chromatic energy imaging combined with the use of iodine-based materials gives single-energy spectral CT a greater ability to detect tiny hemorrhages in the GI than conventional MDCT. In this study, a GE HD750 CT scanner was used for gemstone spectral imaging to confirm its diagnostic value for cases of active bleeding in the GI. Monochromatic energy image spectral CT can detect the less than 0.05 mL/min of bleeding rate, but the digital subtraction angiography could not find it.

### Applications

Monochromatic energy imaging in spectral CT showed superiority over polychromatic energy imaging in detecting GI bleeding. It plays a important role in visualizing tiny hemorrhages in the GI.

### Terminology

MDCT technology has shown increasingly prominent advantages recently in the diagnosis of small bowel bleeding, including energy spectral CT with its advantages of enabling monochromatic energy imaging, reduced tissue attenuation, high resolution, and the detection of tiny changes in tissue density.

### Peer review

This is a good descriptive study in which the authors investigated the value of computed tomography spectral imaging in evaluating the intestinal hemorrhage of 7 different bleeding rates. The results are interesting and suggest that monochromatic energy imaging in spectral CT is a good choice in detecting tiny hemorrhages in the GI.

## REFERENCES

- Dobritz M, Engels HP, Schneider A, Wieder H, Feussner H, Rummeny EJ, Stollfuss JC. Evaluation of dual-phase multi-detector-row CT for detection of intestinal bleeding using an experimental bowel model. *Eur Radiol* 2009; **19**: 875-881 [PMID: 19018538 DOI: 10.1007/s00330-008-1205-5]
- Allison DJ, Hemingway AP, Cunningham DA. Angiography in gastrointestinal bleeding. *Lancet* 1982; **2**: 30-33 [PMID: 6123759 DOI: 10.1016/S0140-6736(82)91162-X]
- Imdahl A, Salm R, Rückauer K, Farthmann EH. [Diagnosis and management of lower gastrointestinal hemorrhage. Retrospective analysis of 233 cases]. *Langenbecks Arch Chir* 1991; **376**: 152-157 [PMID: 1870364 DOI: 10.1007/BF00250340]
- Filippone A, Cianci R, Milano A, Pace E, Neri M, Cotroneo AR. Obscure and occult gastrointestinal bleeding: comparison of different imaging modalities. *Abdom Imaging* 2012; **37**: 41-52 [PMID: 21912990 DOI: 10.1007/s00261-011-9802-1]
- Ernst O, Bulois P, Saint-Drenant S, Leroy C, Paris JC, Sergeant G. Helical CT in acute lower gastrointestinal bleeding. *Eur Radiol* 2003; **13**: 114-117 [PMID: 12541118 DOI: 10.1007/s00330-002-1442-y]
- Coursey CA, Nelson RC, Boll DT, Paulson EK, Ho LM, Neville AM, Marin D, Gupta RT, Schindera ST. Dual-energy multidetector CT: how does it work, what can it tell us, and when can we use it in abdominopelvic imaging? *Radiographics* 2010; **30**: 1037-1055 [PMID: 20631367 DOI: 10.1148/rg.304095175]
- Wang L, Liu B, Wu XW, Wang J, Zhou Y, Wang WQ, Zhu XH, Yu YQ, Li XH, Zhang S, Shen Y. Correlation between CT attenuation value and iodine concentration in vitro: discrepancy between gemstone spectral imaging on single-source dual-energy CT and traditional polychromatic X-ray imaging. *J Med Imaging Radiat Oncol* 2012; **56**: 379-383 [PMID: 22883644 DOI: 10.1111/j.1754-9485.2012.02379.x]
- Horton KM, Fishman EK. The current status of multidetector row CT and three-dimensional imaging of the small bowel. *Radiol Clin North Am* 2003; **41**: 199-212 [PMID: 12659334 DOI: 10.1016/S0033-8389(02)00121-5]
- Boudiaf M, Jaff A, Soyer P, Bouhnik Y, Hamzi L, Rymer R. Small-bowel diseases: prospective evaluation of multi-detector row helical CT enteroclysis in 107 consecutive patients. *Radiology* 2004; **233**: 338-344 [PMID: 15459329 DOI: 10.1148/radiol.2332030308]
- Yoon W, Jeong YY, Shin SS, Lim HS, Song SG, Jang NG, Kim JK, Kang HK. Acute massive gastrointestinal bleeding: detection and localization with arterial phase multi-detector row helical CT. *Radiology* 2006; **239**: 160-167 [PMID: 16484350 DOI: 10.1148/radiol.2383050175]
- Roy-Choudhury SH, Karandikar S. Multidetector CT of acute gastrointestinal bleeding. *Radiology* 2008; **246**: 336 [PMID: 18096554 DOI: 10.1148/radiol.2461070434]
- Dobritz M, Engels HP, Schneider A, Bauer J, Rummeny EJ. Detection of intestinal bleeding with multi-detector row CT in an experimental setup. How many acquisitions are necessary? *Eur Radiol* 2009; **19**: 2862-2869 [PMID: 19588146 DOI: 10.1007/s00330-009-1510-7]
- Johnson TR, Krauss B, Sedlmair M, Graser M, Bruder H, Morhard D, Fink C, Weckbach S, Lenhard M, Schmidt B, Flohr T, Reiser MF, Becker CR. Material differentiation by dual energy CT: initial experience. *Eur Radiol* 2007; **17**: 1510-1517 [PMID: 17151859 DOI: 10.1007/s00330-006-0517-6]
- Wu HW, Cheng JJ, Li JY, Yin Y, Hua J, Xu JR. Pulmonary embolism detection and characterization through quantitative iodine-based material decomposition images with spectral computed tomography imaging. *Invest Radiol* 2012; **47**: 85-91 [PMID: 22107805 DOI: 10.1097/RLI.0b013e31823441a1]
- Yamaguchi T, Yoshikawa K. Enhanced CT for initial localization of active lower gastrointestinal bleeding. *Abdom Imaging* 2003; **28**: 634-636 [PMID: 14628865 DOI: 10.1007/s00261-002-0099-y]
- Wu LM, Xu JR, Yin Y, Qu XH. Usefulness of CT angiography in diagnosing acute gastrointestinal bleeding: a meta-analysis. *World J Gastroenterol* 2010; **16**: 3957-3963 [PMID: 20712058 DOI: 10.3748/wjg.v16.i31.3957]
- Fang JF, Chen RJ, Wong YC, Lin BC, Hsu YB, Kao JL, Kao YC. Pooling of contrast material on computed tomography mandates aggressive management of blunt hepatic injury. *Am J Surg* 1998; **176**: 315-319 [PMID: 9817246 DOI: 10.1016/S0002-9610(98)00196-2]
- Martí M, Artigas JM, Garzón G, Alvarez-Sala R, Soto JA. Acute lower intestinal bleeding: feasibility and diagnostic performance of CT angiography. *Radiology* 2012; **262**: 109-116 [PMID: 22084211 DOI: 10.1148/radiol.11110326]
- García-Blázquez V, Vicente-Bártulos A, Olavarria-Delgado A, Plana MN, van der Winden D, Zamora J. Accuracy of CT angiography in the diagnosis of acute gastrointestinal bleeding: systematic review and meta-analysis. *Eur Radiol* 2013; **23**: 1181-1190 [PMID: 23192375 DOI: 10.1007/s00330-012-2721-x]
- Yeh BM, Shepherd JA, Wang ZJ, Teh HS, Hartman RP, Prevrhal S. Dual-energy and low-kVp CT in the abdomen. *AJR Am J Roentgenol* 2009; **193**: 47-54 [PMID: 19542394 DOI: 10.2214/AJR.09.2592]
- Fletcher JG, Takahashi N, Hartman R, Guimaraes L, Huprich JE, Hough DM, Yu L, McCollough CH. Dual-energy and dual-source CT: is there a role in the abdomen and pelvis? *Radiol Clin North Am* 2009; **47**: 41-57 [PMID: 19195533 DOI: 10.1016/j.rcl.2008.10.003]
- Marin D, Nelson RC, Samei E, Paulson EK, Ho LM, Boll DT, DeLong DM, Yoshizumi TT, Schindera ST. Hypervascular liver tumors: low tube voltage, high tube current multidetector CT during late hepatic arterial phase for detection--initial clinical experience. *Radiology* 2009; **251**: 771-779 [PMID: 19346514 DOI: 10.1148/radiol.2513081330]
- Macari M, Spieler B, Kim D, Graser A, Megibow AJ, Babb J, Chandarana H. Dual-source dual-energy MDCT of pancreatic adenocarcinoma: initial observations with data generated at 80 kVp and at simulated weighted-average 120 kVp. *AJR Am J Roentgenol* 2010; **194**: W27-W32 [PMID: 20028887 DOI: 10.2214/AJR.09.2737]
- Matsumoto K, Jinzaki M, Tanami Y, Ueno A, Yamada M, Kuribayashi S. Virtual monochromatic spectral imaging

with fast kilovoltage switching: improved image quality as compared with that obtained with conventional 120-kVp CT. *Radiology* 2011; **259**: 257-262 [PMID: 21330561 DOI: 10.1148/radiol.111100978]

25 **Zhang D**, Li X, Liu B. Objective characterization of GE discovery CT750 HD scanner: gemstone spectral imaging mode. *Med Phys* 2011; **38**: 1178-1188 [PMID: 21520830 DOI: 10.1118/1.3551999]

**P-Reviewer:** Kurtoglu E, Luo HS, Quattrocchi CC, Syam AF, Yu B  
**S-Editor:** Gou SX **L-Editor:** A **E-Editor:** Liu XM





Published by **Baishideng Publishing Group Inc**  
8226 Regency Drive, Pleasanton, CA 94588, USA  
Telephone: +1-925-223-8242  
Fax: +1-925-223-8243  
E-mail: [bpgooffice@wjgnet.com](mailto:bpgooffice@wjgnet.com)  
Help Desk: <http://www.wjgnet.com/esps/helpdesk.aspx>  
<http://www.wjgnet.com>



ISSN 1007-9327

